Tribol Lett (2013) 49:95–102
DOI 10.1007/s11249-012-0048-z

ORIGINAL PAPER

Plasmonic Diagnostics for Tribology: In Situ Observations Using Surface Plasmon Resonance in Combination with Surface-Enhanced Raman Spectroscopy

Brandon A. Krick · David W. Hahn · W. Gregory Sawyer

Received: 12 March 2012 / Accepted: 15 September 2012 / Published online: 30 September 2012

Abstract The generation of transfer films is a common wear and lubrication mechanism of solid lubricants, such as polymers and lamellar solids. Material can transfer from a solid lubricant to a counter surface as early as the first cycle of sliding, initiating the formation of a transfer film, which can persist for the duration of sliding. Surface plasmon resonance (SPR) was used to monitor incipient molecular wear of a solid lubricant as performed here using a gold coated (50 nm) quartz prism in situ during sliding experiments. Surface-enhanced Raman spectroscopy (SERS) is a complementary technique enabling the analysis of ultra-thin transfer films. SPR and SERS experiments confirm that polytetrafluoroethylene and graphite transfer readily, with observed changes in SPR signal after one cycle of sliding, while ultra-high-molecular-weight polyethylene shows little transfer to the gold during sliding in the in situ SPR experiment. This shows the feasibility of SPR and SERS as important diagnostic tools for tribological studies.

Keywords Surface plasmon resonance (SPR) · Surface-enhanced Raman spectroscopy (SERS) · Polytetrafluoroethylene (PTFE) · Molecular wear · Transfer film · Plasmonics · In situ

1 Introduction and Background

Friction and wear involve many complex interactions within interfaces buried between contacting surfaces; fundamental studies of friction and wear can benefit significantly from complementary analytical tools specifically aimed to interrogate interactions at the buried interface of two solids [1–3]. Tribology has a rich history and even more promising opportunity for applications of analytical and in situ techniques [1–30].

One complexity of tribological system is the concept of the transfer film (i.e., removal of material from one mating surface and subsequent deposition on the opposing surface). This may entail material movement from the molecular scale upward, while temporal scales span from chemical kinetic rates to hours and days [9, 13–16, 20, 23, 24, 31–38]. Analytical techniques, including atomic force microscopy, optical profilometry and microscopy for monitoring and quantifying transfer film and third body formation have their respective advantages and disadvantages; the considerable footprint, relatively long analysis times, resolution limitations on optical techniques, and lack of in situ capabilities of these instruments remain limiting factors [2]. We, therefore, focus on complementary analytical tools specifically aimed to interrogate the buried interfaces with goals of elucidating the temporal and spatial scales of surface kinetics and material transfer by developing an in situ surface plasmon resonance (SPR) tribometer.

Until recently, spectroscopy techniques with single molecule sensitivity have been precluded from in situ tribological efforts [2]. SPR appears to be uniquely suited to provide such high fidelity measurements within a tribological apparatus. In this paper, SPR was used for in situ tribological studies of the dynamics of transfer films of polytetrafluoroethylene (PTFE), ultra-high-molecular-weight polyethylene (UHMWPE), and graphite. This approach offers the ability for in situ investigation of the development of incipient transfer films (ideally at the molecular or near-molecular level), providing experimental capabilities unavailable to date in the tribological

B. A. Krick (✉) · D. W. Hahn · W. G. Sawyer
Department of Mechanical and Aerospace Engineering, University of Florida, Gainesville, FL 32611, USA
e-mail: bakrick@ufl.edu

community. For example, the transfer of discrete fundamental wear units (e.g., molecules, macromolecules, and nano-particulates) is of key importance in understanding the underlying physics and origins of wear processes.

Additionally, surface-enhanced Raman spectroscopy (SERS) is ideally suited to analyze the chemical identity of transfer films generated during in situ SPR experiments. This can confirm the presence and chemical identity of a transfer film and complement the results of the SPR studies. Furthermore, it shows promise to be used for in situ tribology experiments with similar light pathways used for prior in situ optical and Raman experiments [2–4, 6, 10, 13–15, 18–20, 23, 26, 27] and the present in situ SPR experiment.

1.1 Surface Plasmon Resonance

A surface plasmon can be described as a fluctuating electron density wave that propagates parallel and along the boundary of a metal and a dielectric medium [39–42]. The surface plasmon phenomenon was first described to explain unexpected attenuation in diffraction gratings over a century ago [43]. A surface plasmon can be excited by light, in which the energy of a photon is transferred into the electrons of the metal, thereby propagating itself as a surface plasmon. In order for this to occur, the metal must possess conduction band electrons that resonate with the exciting photons. Many types of metals contain the properties to produce surface plasmons (e.g., copper, titanium, chromium, silver, and others), however, gold is often the most suitable. Since this is a surface phenomenon in which both mediums play a role, any slight perturbation to the boundary can greatly alter the induction and propagation of a surface plasmon. For this reason, surface plasmon resonance is a technique which is very sensitive in detecting adsorbed materials on the metal surface, including the detection of mono-layers and single nanoparticles [39, 40, 44].

A simple schematic of the Kretschmann configuration [45] can be seen in Fig. 1. In such configurations, a thin metal film is deposited on one surface of a prism. The prism's high refractive index acts to condition the incoming light ray, changing its wave function so that coupling into a surface plasmon is possible. The angle dependence in the wave function through a prism is such that the plasmon will only be induced at a specific incidence angle, α, characterized by a near total attenuation of the reflected ray.

When the appropriate incident angle is reached and a surface plasmon is generated, reflectance of the incident light is greatly reduced as the majority of the light energy is coupled into the surface plasmon propagating along the

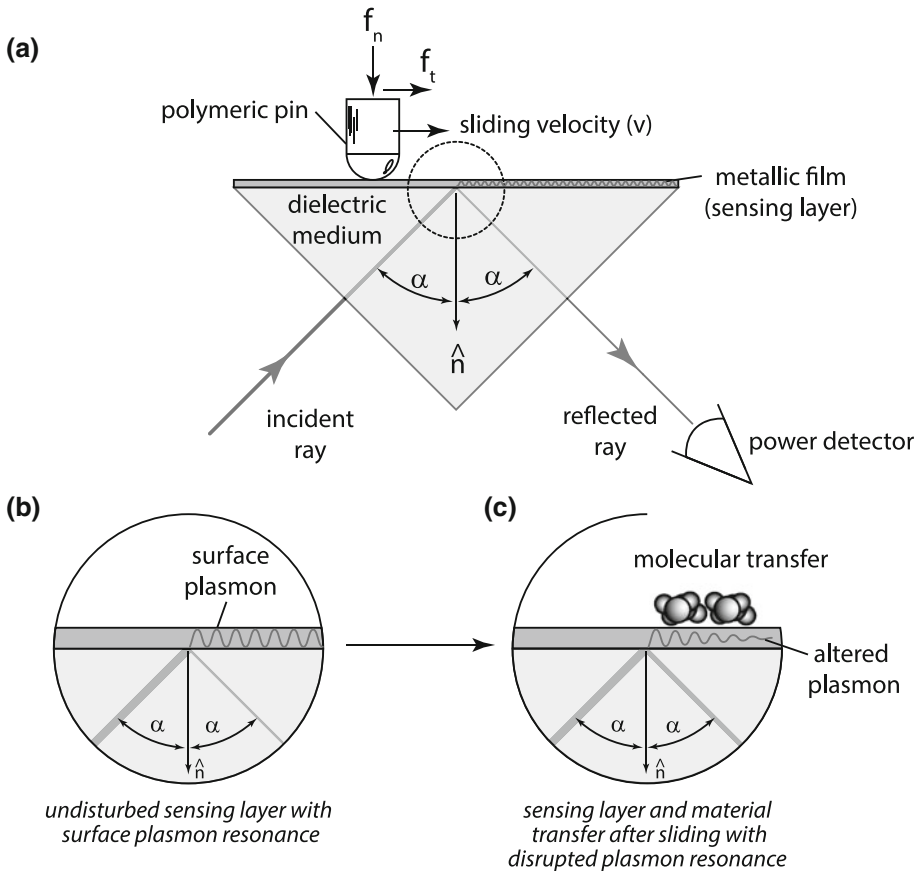

Fig. 1 In situ surface plasmon resonance tribometry. **a** Schematic for in situ surface plasmon resonance tribometer that slides a sample across the metallic film sensing layer on a quartz prism utilizing the Kretschmann configuration. **b** Schematic of the Kretschmann configuration for generation of a surface plasmon. **c** Schematic of the modification of the surface plasmon due to molecular adsorbates or transfer on the metallic sensing layer

metal and dielectric interface. As material becomes adsorbed (e.g., a monolayer) onto the surface of the metal opposite the plasmon, the angle, α, at which resonance occurs is altered. This allows for a measurement of reflectance intensity versus incident angle to be made indicating changes due to adsorbed material at the surface of the metal. Alternatively, one may expand the incident beam to cover a large surface area and then tune the incident angle to plasmon resonance, and an image may be recorded of the reflected beam. Any changes to the sensing surface are detected by changes in intensity of the reflected image as the surface plasmon is disrupted by adsorbed analyte [44]. As described above, since the surface plasmon is so highly dependent on the interface, measureable differences in reflectance will occur due to the smallest perturbations to the boundary, allowing for very sensitive surface measurements.

We note that the SPR technique generally responds to refractive index changes on the sensing layer to a depth of a few hundred nanometers. Jung et al. explored the interpretation of the SPR surface response in the context of quantifying the thickness or surface concentration of an adsorbed layer, including calculations of the SPR angle as a function of adsorbed layer thickness for various refractive index pairs, and assessing the effect of refractive index change on the SPR wavelength. For a bulk refractive index mismatch of 0.1, detection limits for an adsorbed layer thickness are estimated to be sub-angstrom [46]. Kooyman et al.[47] also examine the sensitivity of SPR sensors in the context of sensing layer thickness.

Here, the SPR method was implemented into an in situ tribometer to monitor transfer from solid lubricant materials to a gold coated quartz prism. Increases in reflected intensity of the incident beam at a fixed incident angle correspond to molecular transfer from the solid lubricant sample to the gold sensing surface.

1.2 Surface-Enhanced Raman Spectroscopy

Raman spectroscopy is an inelastic-scattering molecular probe (i.e., vibrational spectroscopy) that is readily implemented with a single excitation laser source. The Raman effect arises from coupling of the EM wave-induced dipole moment with the vibrational quanta of the targeted analyte. While a very versatile spectroscopic tool, Raman scattering is characterized by very low scattering cross sections that limit applicability. These limitations may be overcome with surface-enhanced Raman spectroscopy, in which surface plasmons, primarily on the surfaces of gold and silver, interact with an adjacent or adsorbed analyte to boost the Raman signal by orders of magnitude in many cases, including factors greater than 10^6 for single molecules [48]. The physics of the SERS effect is rooted in the localized surface plasmons created by the incident laser beam on the SERS substrate, which we consider here in terms of the classical electromagnetic field effect [48–50]. Silver and gold are the most common choices for the SERS substrate because visible excitation wavelengths (e.g., 488, 514, and 632 nm laser lines) effectively couple to the resonance plasmon frequencies. The localized electric field is then greatly increased by the surface plasmon, which subsequently increases the field that interacts with a targeted analyte molecule adsorbed to the substrate surface, thereby enhancing the Raman scattering through the induced-dipole interactions. Surface roughness and curvature can influence the surface plasmon and resulting SERS enhancement, as edge effects can greatly alter the EM field enhancement.

2 Materials

2.1 Gold Coated Quartz Prisms

Counterfaces for in situ SPR experiments were gold coated quartz prisms. The prisms were right angle triangular prisms defined by a right triangle with a 35.36 mm hypotenuse and 25 mm legs. A 5 nm chromium bond layer and a 50 nm gold layer were coated on the hypotenuse face of the prism.

2.2 Polytetrafluoroethylene

Polytetrafluoroethylene (PTFE) is an excellent solid lubricant because of its low friction coefficient (reported between 0.04 and 0.2), its chemical inertness, and its resistance to a wide variety of environments [34, 51–56]. Disadvantages of PTFE include its high wear rate ($\sim 1 \times 10^{-4}$ to 1×10^{-3} mm^3/Nm [57]) and the large amount of wear debris produced [56–58]. PTFE is known to develop a transfer film; although an incubation period for wear has been observed and discussed [34, 56–59], little is understood about this mild-wear incubation process for unfilled material. DuPont Teflon® 7C PTFE was used for in situ SPR experiments. PTFE samples were machined to a tip radius of 1 mm. Samples were washed with soap and water then sonicated in methanol for 30 min and then dried prior to testing.

2.3 Ultra-High-Molecular-Weight Polyethylene (UHMWPE)

Ultra-high-molecular-weight polyethylene is another excellent polymeric candidate for use as a solid lubricant [31, 60–62]; it differs in that its performance is often thought not to require transfer films, but rather smooth

counter surfaces [60]. Pooley and Tabor [61] found that high density polyethylene and "extended chain polyethylene" had noticeably less transfer than PTFE. They also noted that transfer films were observed for PTFE when slid against steel, while no detectable films were observed in the case of polyethylene against steel [61]. This makes UHMWPE an ideal candidate as a negative control for SPR experiments; where there should be minimal increase in reflectivity during SPR experiments. UHMWPE physical properties and friction coefficient are similar to PTFE so the main difference in the experiments should be the amount of transfer measured by SPR. UHMWPE samples were also machined to a 1 mm tip radius. Samples were washed with soap and water, sonicated in methanol for 30 min, and dried prior to testing.

2.4 Graphite

Graphite is commonly used for its ability to transfer and make low friction films. One of its most common uses is in composites used for writing in pencils. The most prevalent composition in pencils is the HB (number 2) pencil, which consists of clay and graphite. This composition is ideal for transfer film experiments in that it is designed to transfer readily and is not too hard to damage the counterface. HB graphite composites were extracted from standard #2 pencils and finished to a tip radius of 1 mm. Samples were rinsed in methanol and then wiped with a clean laboratory wipe.

3 Methods

3.1 In Situ Surface Plasmon Resonance (SPR) Tribometer

SPR was used to monitor transfer film formation as a function of sliding cycle. A linear reciprocating pin on flat tribometer was used to perform friction and SPR measurements. A 632 nm laser with power of 540 mW is transmitted through one leg face of the prism, directed at the hypotenuse (gold coated) face. The reflected intensity of this light is measured through the other leg face of the prism with an optical power meter as shown in Fig. 1. The angle of incidence is adjusted such that the surface plasmon resonance effect is a maximum and the reflected power is a minimum ($\sim$0.005 %). After this, the sample (PTFE, UHMWPE, or graphite) is loaded against the gold surface of the prism and sliding is initiated. After each sliding cycle (one forward and reverse motion), a value of reflected intensity is recorded. An increase in this intensity corresponds to a change in the adsorbates on the gold sensing layer of the prism, which in this case would be material transfer.

The tribometer was designed around the gold coated prism (the counterface) and mounted on a rotational stage. The rotational stage is used to adjust the angle of incidence to tune the initial plasmon effect in the system. The sample (i.e., PTFE, UHMWPE, or graphite) was mounted to a bi-axial cantilever force transducer [63]. The sample was loaded into contact with the gold surface of the prism with a manual micrometer. The beam was 1.6 mm in diameter at the point of contact and was centered on the transfer film at the midpoint of the sliding cycle.

3.2 Surface-Enhanced Raman Spectroscopy (SERS) and Raman Spectroscopy

For all Raman spectroscopy, a fully automated commercial micro-Raman system was used (LabRam Infinity). This system used a 15 mW continuous helium:neon laser (λ = 632.8 nm). A 100$\times$ magnification (N.A. = 0.9) objective was used to focus the laser to a diameter of 5 μm. An internal camera was used to find the region of interest (wear tracks) and neutral density filters were used to adjust the excitation energy of the laser at the sample surface. The scattered light was collected via backscatter by the same microscope objective with elastic scattered light rejected by a sharp-edge filter; it was dispersed by an 1,800 grove/mm grating and imaged by a CCD detector (1,024 $\times$ 256 pixels).

Surface-enhanced Raman was achieved utilizing the micro-Raman system on the transfer films that were deposited on the gold surface of the prism. The gold coating required for the SPR experiments also produced the surface-enhanced scattering effect for spectral analysis. Spectra on transfer films on the gold coating were compared to transfer films on uncoated quartz to validate the SERS effect.

3.3 Optical In Situ Micro-tribometer

A micro-tribometer equipped with an in situ microscope and camera [27] was used to analyze the wear of PTFE when slid against glass. The objective is mounted beneath the contact and focuses through the glass on the contact spot between the glass and PTFE sample. Real contact area, transfer film formation, wear debris formation, and wear debris motion can be observed with the optics as the PTFE is worn by sliding against the glass. The contact spot is a dark spot in the image, while higher order fringes surround the contact and map the near contact separation distance. Furthermore, larger third bodies under the contact are distinguished from the sample contact, as they are outlined with higher order interference fringes.

4 Results

Sliding experiments were performed with a linear velocity of 1 mm/s for PTFE, UHMWPE, and graphite. In an effort to increase material transfer for one experiment, PTFE was heated to phase I (~370 K); heating of PTFE has been shown to increase transfer [59]. An externally applied normal load of 1 N was used for UHMWPE, PTFE (room temperature), and heated PTFE (phase I) experiments while a load of 0.2 N was used for the graphite composite. Figure 2 shows the reflected laser power normalized to the incident laser power as a function of sliding cycle. The arbitrary intensity of the SPR measurement, $\bar{I}$, is equal to the measured intensity, I offset by the initial intensity before sliding, I_0, all normalized by the incident laser intensity, I_{in}, as shown in Eq. 1.

$$\bar{I} = (I - I_0)/I_{in} \quad (1)$$

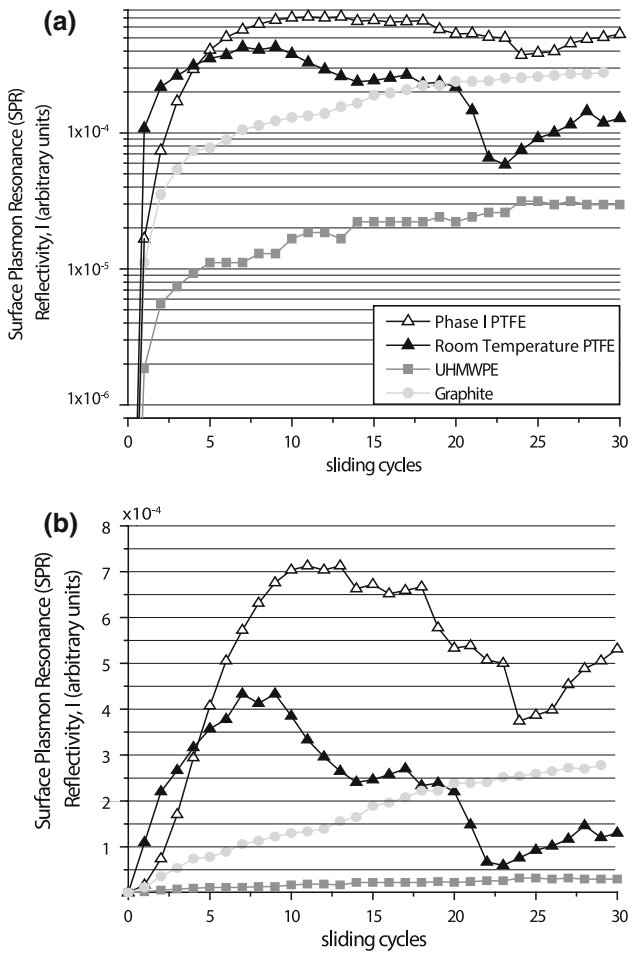

Fig. 2 In situ surface plasmon resonance reflectivity versus sliding cycle for sliding experiments of phase I PTFE, room temperature PTFE, UHMWPE, and graphite. SPR reflectivity intensity measured and calculated by Eq. 1 is shown in **a** log–linear scale and **b** linear–linear for visualization convenience

For both PTFE samples, a strong increase in reflectance is observed, followed by a slow reduction. The graphite sample shows a steady increase in SPR signal with each additional sliding cycle. Minimal increases in surface reflectance were observed in the UHMWPE experiments.

After each experiment, surface-enhanced Raman was performed on each transfer film. For the PTFE and heated PTFE transfer film, a spectrum was observed that is consistent with a bulk PTFE reference (Fig. 3). This can be contrasted with the non-surface-enhanced Raman spectrum of a PTFE transfer film generated by sliding PTFE on quartz (without a gold layer). The graphite track also produced a surface-enhanced Raman spectrum consistent with the graphite reference. No signal outside of the noise was observed for the UHMWPE transfer film. This is consistent with the minimal change in signal observed by the SPR, implying that there was minimal (if any) transfer of UHMWPE.

PTFE was slid against glass in an optical in situ microtribometer. Figure 4 shows a sequence of images collected during sliding. From the images it was observed that a shearing event can produce a transfer filament (Fig. 4c) of PTFE to the glass. The PTFE sample will slide over the PTFE filament for some time without moving the filament (Fig. 4d–g). After several cycles of sliding, the filament may be picked up and moved from its initial transfer location to another location as shown in Fig. 4h.

5 Discussion

5.1 UHMWPE

Minimal changes in surface reflectance were observed in the SPR signal when UHMWPE was slid against gold. The

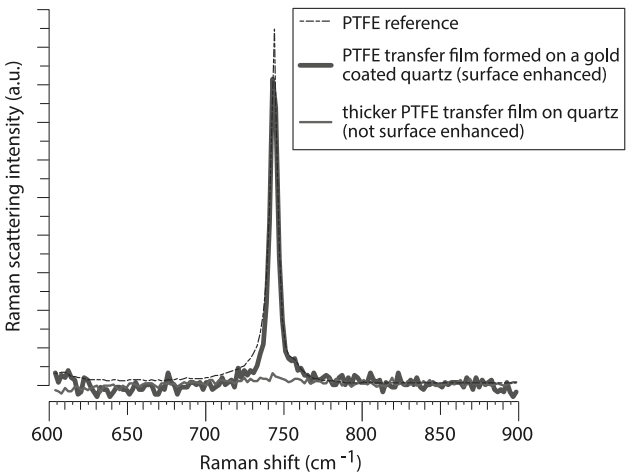

Fig. 3 Surface-enhanced Raman scattering for PTFE transfer film formed during in situ SPR experiments. A PTFE reference spectrum and a spectrum for PTFE transferred to glass by sliding are shown for comparison

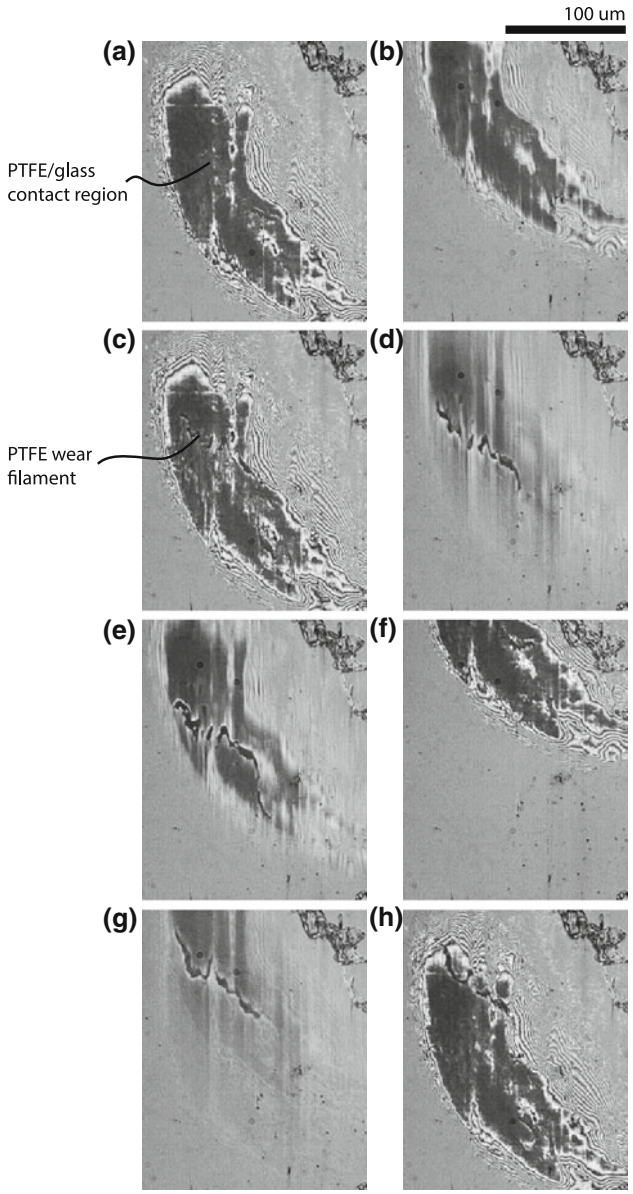

Fig. 4 In situ optical microscopy of PTFE, sliding on glass, and generating a wear filament. Sequential images show: **a** static contact; **b** sliding; **c** static with wear filament in contact; **d; e** sliding over wear filament, **f**; **g** wear filament moved during sliding; **h** wear filament moved to outside of static contact. For all images, the *dark area* is the contact between PTFE and glass. It is surrounded by interference fringes caused by the interference of reflections from the surface of the glass and from the surface of the PTFE in the near contact region

lack of change in intensity implies that the surface plasmon was unaltered during sliding and should be interpreted as UHMWPE sliding without transferring material to the gold layer. Mechanically UHMWPE is very similar to PTFE, with the important difference in the ability to form transfer films at low sliding cycles under these sliding conditions. The nearly unaltered plasmon in the UHMWPE experiments confirms that the mechanical interaction of the polymer and gold did not cause false SPR signal due to mechanical deformation of the gold layer. This further validates that the response of SPR during the sliding of PTFE and similar materials is not simply caused by the wearing or deformation of the gold layer. Additionally, the SERS results confirm that there is no detectable UHMWPE transfer. These tests provide an excellent negative control for in situ SPR tribological experiments.

5.2 Graphite

A monotonic increase in SPR signal is observed when the graphite sample was slid against the gold sensing layer. This increase is consistent with observations of transfer from the graphite sample to the gold in surface-enhanced Raman measurements. This is no surprise, as the graphite composite used in pencils is designed to transfer continuous deposition of graphite with each sliding cycle. Anyone who has ever sketched with a pencil knows that one can darken a line by either pressing harder or by increasing the number of strokes over the line. We also note that preliminary experiments of higher loads ($\sim$1 N) were found to remove the gold layer from the prism.

5.3 PTFE

Large increases in the reflected intensities came in the PTFE systems, with the phase I PTFE (heated) experiment producing the largest change. This large increase in reflectance corresponds to material transfer from the PTFE to the gold layer on the prism and as expected, the phase I PTFE transferred material more readily than room temperature PTFE during sliding. After approximately 10 sliding cycles, the SPR signal decreased, implying a decrease in transferred material on the gold layer in the analysis zone. It has been shown by the results from the optical in situ tribometer (Fig. 4) that PTFE will transfer and the transferred material may be moved around. The transferred material will most likely be moved to and accumulate at the ends of the sliding cycle as shown in the results from sliding PTFE on glass in the optical in situ micro-tribometer. Since the SPR measurements are taking place halfway along the sliding cycle, this accumulation would not be measured; instead there would be some balance of transfer and removal.

The in situ SPR results suggest a new understanding of the first transfer of PTFE and the transition from the mild wear of PTFE. As previously discussed, PTFE wears through a delamination wear process in which subsurface cracks propagate through the polymer and flakey wear debris is ejected. The SPR results suggest that there is also a gradual wear process in which PTFE is transferred in as early as one sliding cycle. This mild transfer mechanism is different than the delamination wear process of PTFE and

is possibly dominated by attractive forces between the PTFE and the metal counterface. Generally, the first sliding cycle of PTFE has higher friction than the sliding cycles immediately following it. This could be a result of the sliding interface changing from PTFE on metal to PTFE on a molecularly thin transfer film of PTFE. As sliding is continued, crack propagations in the subsurface allow debris to be ejected and the system transitions to the poor wear behavior commonly observed in PTFE.

Surface-enhanced Raman confirms the transfer of PTFE to the gold sensing layer. A transfer film of PTFE on quartz is unobservable by traditional Raman spectroscopy. The surface-enhanced effect provided by the gold sensing layer makes it possible to confirm that the increase in surface plasmon resonance is caused by transfer of PTFE. Future incorporation of in situ SERS appears feasible based on the current findings.

6 Concluding Remarks

In situ surface plasmon resonance measurements were used to detect material transfer from PTFE, UHMWPE, and graphite when slid against a gold coated quartz prism. Incipient transfer film formation was observed from PTFE and graphite, while minimal transfer was observed from UHMWPE. Surface-enhanced Raman spectroscopy was used to confirm the chemical identity of transferred species. Furthermore, an in situ optical tribometer was used to explain the increase and subsequent decrease in SPR intensity during sliding of PTFE on gold.

Surface plasmonics such as SPR and SERS are applicable to the field of tribology and show promise for in situ studies of friction and wear. As the use of surface plasmon resonance progresses in tribological studies, future work will be to quantify material transfer as a function of SPR signal. Furthermore, there is a clear opportunity to apply surface-enhanced Raman spectroscopy for in situ tribological studies using the in situ strategies discussed here and throughout the literature.

Acknowledgments The authors thank Kathryn Harris and Jeff Ewin for their assistance in sample preparation, and Bret Windom for the preliminary work on the feasibility of SPR. The authors also acknowledge the University of Florida Microfabritech group for depositing gold coatings for SPR and SERS experiments.

References

1. Martin, J.M., Belin, M.: New trends in analytical tribology. Thin Solid Films **236**, 173–179 (1993)
2. Sawyer, W.G., Wahl, K.J.: Accessing inaccessible interfaces: in situ approaches to materials tribology. MRS Bull. **33**, 1145–1148 (2008)
3. Wahl, K.J., Sawyer, W.G.: Observing interfacial sliding processes in solid–solid contacts. MRS Bull. **33**, 1159–1167 (2008)
4. Sliney, H.E.: Dynamics of solid lubrication as observed by optical microscopy. ASLE Trans. **21**, 109–117 (1978)
5. Berthier, Y., Play, D.: Wear mechanisms in oscillating bearings. Wear **75**, 369–387 (1982)
6. Belin, M., Martin, J.M.: Triboscopy, a new approach to surface degradations of thin films. Wear **156**, 151–160 (1992)
7. McDevitt, N.T., Donley, M.S., Zabinski, J.S.: Utilization of Raman spectroscopy in tribochemistry studies. Wear **166**, 65–72 (1993)
8. Jullien, A., Meurisse, M.H., Berthier, Y.: Determination of tribological history and wear through visualisation in lubricated contacts using a carbon-based composite. Wear **194**, 116–125 (1996)
9. Singer, I.L., LeMogne, T., Donnet, C., Martin, J.M.: In situ analysis of the tribochemical films formed by SiC sliding against Mo in partial pressures of SO_2, O_2, and H_2S gases. J. Vac. Sci. Technol. A: Vac. Surf. Films **14**, 38–45 (1996)
10. Wahl, K.J., Belin, M., Singer, I.L.: A triboscopic investigation of the wear and friction of MoS_2 in a reciprocating sliding contact. Wear **214**, 212–220 (1998)
11. Cheong, C.U.A., Stair, P.C.: In situ studies of the lubricant chemistry and frictional properties of perfluoropolyalkyl ethers at a sliding contact. Tribol. Lett. **10**, 117–126 (2001)
12. Dvorak, S.D., Wahl, K.J., Singer, I.L.: Friction behavior of boric acid and annealed boron carbide coatings studied by in situ Raman tribometry. Tribol. Trans. **45**, 354–362 (2002)
13. Scharf, T.W., Singer, I.L.: Role of third bodies in friction behavior of diamond-like nanocomposite coatings studied by in situ tribometry. Tribol. Trans. **45**, 363–371 (2002)
14. Scharf, T.W., Singer, I.L.: Monitoring transfer films and friction instabilities with in situ Raman tribometry. Tribol. Lett. **14**, 3–8 (2003)
15. Scharf, T.W., Singer, I.L.: Quantification of the thickness of carbon transfer films using Raman tribometry. Tribol. Lett. **14**, 137–145 (2003)
16. Singer, I.L., Dvorak, S.D., Wahl, K.J., Scharf, T.W.: Role of third bodies in friction and wear of protective coatings. J. Vac. Sci. Technol. A: Vac. Surf. Films **21**, S232–S240 (2003)
17. Bae, S.C., Lee, H., Lin, Z.Q., Granick, S.: Chemical imaging in a surface forces apparatus: confocal Raman spectroscopy of confined poly(dimethylsiloxane). Langmuir **21**, 5685–5688 (2005)
18. Cann, P.M., Spikes, H.A.: In-contact IR spectroscopy of hydrocarbon lubricants. Tribol. Lett. **19**, 289–297 (2005)
19. Ovcharenko, A., Halperin, G., Etsion, I., Varenberg, M.: A novel test rig for in situ and real time optical measurement of the contact area evolution during pre-sliding of a spherical contact. Tribol. Lett. **23**, 55–63 (2006)
20. Chromik, R.R., Baker, C.C., Voevodin, A.A., Wahl, K.J.: In situ tribometry of solid lubricant nanocomposite coatings. Wear **262**, 1239–1252 (2007)
21. Hu, J.J., Wheeler, R., Zabinski, J.S., Shade, P.A., Shiveley, A., Voevodin, A.A.: Transmission electron microscopy analysis of Mo–W–S–Se film sliding contact obtained by using focused ion beam microscope and in situ microtribometer. Tribol. Lett. **32**, 49–57 (2008)
22. Marks, L.D., Warren, O.L., Minor, A.M., Merkle, A.P.: Tribology in full view. MRS Bull. **33**, 1168–1173 (2008)
23. Wahl, K.J., Chromik, R.R., Lee, G.Y.: Quantitative in situ measurement of transfer film thickness by a Newton's rings method. Wear **264**, 731–736 (2008)
24. Merkle, A.P., Erdemir, A., Eryilmaz, O.L., Johnson, J.A., Marks, L.D.: In situ TEM studies of tribo-induced bonding modifications in near-frictionless carbon films. Carbon **48**, 587–591 (2010)
25. Dudder, G., Zhao, X., Krick, B., Sawyer, W., Perry, S.: Environmental effects on the tribology and microstructure of MoS_2–Sb_2O_3–C films. Tribol. Lett. **42**, 203–213 (2011)

26. Muratore, C., Bultman, J.E., Aouadi, S.M., Voevodin, A.A.: In situ Raman spectroscopy for examination of high temperature tribological processes. Wear **270**, 140–145 (2011)
27. Krick, B., Vail, J., Persson, B., Sawyer, W.: Optical in situ micro tribometer for analysis of real contact area for contact mechanics, adhesion, and sliding experiments. Tribol. Lett. **45**, 185–194 (2012)
28. Lorenz, B., Persson, B.N.J., Dieluweit, S., Tada, T.: Rubber friction: comparison of theory with experiment. Eur. Phys. J. E **34**, 1–11 (2011)
29. Murarash, B., Varenberg, M.: Tribometer for in situ scanning electron microscopy of microstructured contacts. Tribol. Lett. **41**, 319–323 (2011)
30. Etsion, I.: Discussion of the paper: optical in situ micro tribometer for analysis of real contact area for contact mechanics, adhesion, and sliding experiments. Tribol. Lett. **46**, 205 (2012)
31. Blanchet, T.A., Kennedy, F.E.: The development of transfer films in ultra-high molecular weight polyethylene/stainless steel oscillatory sliding. Tribol. Trans. **32**, 371–379 (1989)
32. Blanchet, T.A., Kennedy, F.E., Jayne, D.T.: XPS analysis of the effect of fillers on PTFE transfer film development in sliding contacts. Tribol. Trans. **36**, 535–544 (1993)
33. Gong, D.L., Zhang, B., Xue, Q.J., Wang, H.L.: Effect of tribochemical reaction of polytetrafluoroethylene transferred film with substrates on its wear behaviour. Wear **137**, 267–273 (1990)
34. Makinson, K.R., Tabor, D.: Friction and transfer of polytetrafluoroethylene. Nature **201**, 464–466 (1964)
35. Pooley, C.M., Tabor, D.: Transfer of PTFE and related polymers in a sliding experiment. Nat. Phys. Sci. **237**, 88–90 (1972)
36. Sinnott, S.B., Jang, I., Phillpot, S.R., Dickrell, P.L., Burris, D.L., Sawyer, W.G.: Mechanisms responsible for the tribological properties of PTFE transfer films. Abstr. Pap. Am. Chem. Soc. **231**, 23 (2006)
37. Sawyer, W.G., Perry, S.S., Phillpot, S.R., Sinnott, S.B.: Integrating experimental and simulation length and time scales in mechanistic studies of friction. J. Phys. Condens. Matter **20**, 354012 (2008)
38. Liu, Y., Erdemir, A., Meletis, E.I.: A study of the wear mechanism of diamond-like carbon films. Surf. Coat. Technol. **82**, 48–56 (1996)
39. Homola, J.: Present and future of surface plasmon resonance biosensors. Anal. Bioanal. Chem. **377**, 528–539 (2003)
40. Homola, J., Yee, S.S., Gauglitz, G.: Surface plasmon resonance sensors: review. Sens. Actuators B-Chem. **54**, 3–15 (1999)
41. Li Y.J.: Adsorption processes and spatiotemporal pattern formation during electrochemical reactions on Au(111) film electrodes, a surface plasmon resonance study. Dissertation, Freie Universitat Berlin (2003)
42. Yee, S.S., Homola, J., Gauglitz, G.: Special issue: surface plasmon resonance (SPR) optical sensors, current technology and applications—preface. Sens. Actuators B-Chem. **54**, 1 (1999)
43. Wood, R.W.: On a remarkable case of uneven distribution of light in a diffraction grating spectrum. Philos. Mag. **4**, 396–402 (1902)
44. Zybin, A., Kuritsyn, Y., Gurevich, E., Temchura, V., Überla, K., Niemax, K.: Real-time detection of single immobilized nanoparticles by surface plasmon resonance imaging. Plasmonics **5**, 31–35 (2010)
45. Kretschmann, E.: Decay of non radiative surface plasmons into light on rough silver films. comparison of experimental and theoretical results. Opt. Commun. **6**, 185–187 (1972)
46. Jung, L.S., Campbell, C.T., Chinowsky, T.M., Mar, M.N., Yee, S.S.: Quantitative interpretation of the response of surface plasmon resonance sensors to adsorbed films. Langmuir **14**, 5636–5648 (1998)
47. Kooyman, R.P.H., Kolkman, H., Van Gent, J., Greve, J.: Surface plasmon resonance immunosensors: sensitivity considerations. Anal. Chim. Acta **213**, 35–45 (1988)
48. Xu, H.X., Aizpurua, J., Kall, M., Apell, P.: Electromagnetic contributions to single-molecule sensitivity in surface-enhanced Raman scattering. Phys. Rev. E **62**, 4318–4324 (2000)
49. Campion, A., Kambhampati, P.: Surface-enhanced Raman scattering. Chem. Soc. Rev. **27**, 241–250 (1998)
50. Kambhampati, P., Child, C.M., Foster, M.C., Campion, A.: On the chemical mechanism of surface enhanced Raman scattering: experiment and theory. J. Chem. Phys. **108**, 5013–5026 (1998)
51. Flom, D.G., Porile, N.T.: Friction of teflon sliding on teflon. J. Appl. Phys. **26**, 1088–1092 (1955)
52. Flom, D.G., Porile, N.T.: Effects of temperature and high-speed sliding on the friction of teflon on teflon. Nature **175**, 682 (1955)
53. Hanford, W.E., Joyce, R.M.: Polytetrafluoroethylene. J. Am. Chem. Soc. **68**, 2082–2085 (1946)
54. Renfrew, M.M., Lewis, E.E.: Polytetrafluoroethylene—heat-resistant, chemically inert plastic. Ind. Eng. Chem. **38**, 870–877 (1946)
55. Shooter, K.V., Tabor, D.: The frictional properties of plastics. Proc. Phys. Soc. Lond. Sect. B **6**(5), 661 (1952)
56. Tanaka, K., Uchiyama, Y., Toyooka, S.: Mechanism of wear of polytetrafluoroethylene. Wear **23**, 153–172 (1973)
57. Blanchet, T.A., Kennedy, F.E.: Sliding wear mechanism of polytetrafluoroethylene (PTFE) and PTFE composites. Wear **153**, 229–243 (1992)
58. Biswas, S.K., Vijayan, K.: Friction and wear of PTFE—a review. Wear **158**, 193–211 (1992)
59. Yang, E.L., Hirvonen, J.P., Toivanen, R.O.: Effect of temperature on the transfer film formation in sliding contact of PTFE with stainless steel. Wear **146**, 367–376 (1991)
60. Barrett, T.S., Stachowiak, G.W., Batchelor, A.W.: Effect of roughness and sliding speed on the wear and friction of ultra-high molecular weight polyethylene. Wear **153**, 331–350 (1992)
61. Pooley, C.M., Tabor, D.: Friction and molecular structure: the behaviour of some thermoplastics. Proc. R. Soc. Lond. Ser. A, Math. Phys. Sci. **329**, 251–274 (1972)
62. Welghtman, B., Light, D.: The effect of the surface finish of alumina and stainless steel on the wear rate of UHMWPE polyethylene. Biomaterials **7**, 20–24 (1986)
63. Krick, B.A., Sawyer, W.G.: Space tribometers: design for exposed experiments on orbit. Tribol. Lett. **41**, 303–311 (2011)